Versatility of dislocation motions in polycrystalline UO2 deformed at 1550 °C investigated by TEM

C. Onofri, J.P. Monchoux, J. Amodeo, R. Madec, C. Sabathier, H. Palancher, J. Fouet, D. Drouan, M. Legros

C. Onofri, J.P. Monchoux, J. Amodeo, R. Madec, C. Sabathier, H. Palancher, J. Fouet, D. Drouan, M. Legros, Scripta Materialia 244 (2024) 116034. https://doi.org/10.1016/j.scriptamat.2024.116034.

Versatility of dislocation motions in polycrystalline UO_2 deformed at 1550°C investigated by TEM

C. Onofri[a*], J.P. Monchoux[b], J. Amodeo[c], R. Madec[d,e], C. Sabathier[a], H. Palancher[a], J. Fouet[a], D. Drouan[a], M. Legros[b]

[a] CEA, DES, IRESNE, DEC, Cadarache, F-13108 Saint Paul Lez Durance, France
[b] CEMES, CNRS, 29 rue Jeanne Marvig, 31055 Toulouse Cedex 4, France
[c] Aix Marseille Université, Université de Toulon, CNRS, IM2NP, 13397 Marseille, France
[d] CEA, DAM, DIF, F-91297 Arpajon, France
[e] Université Paris-Saclay, CEA, Laboratoire Matière en Conditions Extrêmes, F-91680 Bruyères-le-Châtel, France

*Corresponding author: claire.onofri@cea.fr
Key words: *uranium dioxide (UO_2), dislocations, transmission electron microscopy (TEM), mechanical test*

Abstract

The present study explores the behavior of dislocations in uranium dioxide (UO_2) under mechanical loading at high-temperature. Transmission electron microscopy characterization was carried out on polycrystalline UO_2 pellets after uniaxial compression tests performed at constant strain rate and 1550°C. The detailed characterization of dislocation motion provides insights on the deformation processes operating at the nanoscale that are critical to better understand the viscoplastic response of the UO_2 nuclear fuel during off-normal power transient. Results emphasize the complexity of dislocation motion at high temperature since it involves glide and a mixed mechanism involving climb, called mixed climb, which was not evidenced earlier in this material.

Uranium dioxide (UO_2, fluorite structure) is the most common nuclear fuel material for pressurized water reactors (PWRs). To this aim, UO_2 is sintered into cylindrical pellets which are stacked in a zirconium alloy cladding tube. One of the main safety issues for reactor operation is to ensure the mechanical integrity of this cladding, which is the first barrier ensuring the fuel confinement, and this under all operating conditions, i.e. normal and off-normal. During in-pile irradiation, different physical phenomena (pellet thermal and irradiation expansion, compressive stress applied by the pressurized water onto the cladding…) contribute to the progressive closure of the initial gap between the pellet and the cladding [1]. This local mechanical pellet-to-cladding interaction can be further accentuated during off-normal power transients, characterized by a high-power rise within a time frame of about a few tens of milliseconds to several minutes. Under such conditions, significant stresses associated to high temperature accelerate the viscoplastic deformation of the pellet center, *i.e.* a region where temperature can reach elevated values which depend on the exact scenario but are typically estimated between 1200 and more than 2000°C. The viscoplastic behavior of the fuel material plays thus a key role to accommodate the pellet volume expansion during normal and off-normal operating conditions of such nuclear power reactors. However, it is a complex process due to the heterogeneous fuel microstructure and its evolution under irradiation.

The deformation mechanisms of UO_2 were extensively studied in the literature mostly relying on uniaxial compression tests (with a constant load or strain rate) mainly performed on polycrystalline pellets [2][3][4][5][6][7][8][9][10][11][12][13][14][15][16][17][18][19][20]. A more limited amount of studies was also done on single crystals [13][21][22][23][24][25]. Different temperature (*T*), strain rate ($\dot{\varepsilon}$) and stress (σ) conditions are reported. Those $\dot{\varepsilon}$, σ and *T* are usually rationalized using a power law for stress sensitivity and an Arrhenius law for thermal activation. Under secondary creep conditions,

most of the studies propose two regimes for the viscoplastic behavior of UO_2 pellets [2][3] characterized by a transition stress (σ_t) value that varies with several parameters such as stoichiometry [4][5], material density [2], grain size [3][6] and temperature [7]. Below σ_t (referred to as low stress domain), the strain rate varies rather linearly with the applied stress, which is usually considered as an indication that a diffusional creep mechanism (such as Nabarro-Herring or Coble mechanism) is involved [8]. Above this transition stress (referred to as high stress domain), the strain rate varies as a power of the stress with an exponent n varying between 4 and 5, suggesting a mechanism based on dislocation motion [9][10]. Some authors also described the viscoplastic behavior by a unique hyperbolic sine law for a wide range of stresses, involving dislocation motion and grain boundary sliding [11][12].

As observed in other crystalline materials, dislocation motion in UO_2 can rely on different mechanisms depending on temperature, applied stress, and strain rate. A few experimental studies focusing on the dislocation microstructure generated during deformation tests exist. Between 750 and 1150°C, on single crystals, Alamo *et al.* [26] and Yust *et al.* [27] observed dislocation dipoles, structures that look like superjogs, entangled lines and also long lines that present sharp changes from one <100> direction to another one (forming cups), using transmission electron microscopy (TEM). All these observations suggest a glide-type dislocation motion. In this temperature range, dislocation glide is controlled by the state of stress applied to the grain and is confined in small set of planes as suggested by Yust *et al*. [28]. In polycrystalline samples, they observed that dislocations interact with obstacles, like manufacturing porosities or grain boundaries, that lead to an increase of internal stress and premature failure. In those polycrystalline samples, only glide in the {100} planes is assumed to be active in this temperature range inducing an inhomogeneous repartition of dislocations between the grains [28]. More generally, in UO_2, three slip modes were identified: {001}, {110} and {111}, all characterized by the same Burgers vector ½<110> [26][27][29][24][21][25]. Critical resolved shear stress (CRSS) was measured in both ½<110>{001} and ½<110>{110} slip modes and showed significant variations with temperature attributed to the lattice friction and dislocation core structure up to a critical transition temperature ($T_a^{\{hkl\}}$) [30][31][32][33]. The ½<110>{001} slip system is the most favorable slip mode as having the lower CRSS below $T_a^{\{001\}}$ when compared to ½<110>{110} that is activated at larger stress [29][21][34][13][23]. No CRSS can be found for ½<110>{111} since it has never been tested independently from the two other slip modes in stoichiometric UO_2. For this latter, dislocation observations were attributed to cross slip from {100} and {110} [24][21][26][35]. Furthermore, the U/O ratio also influences the slip mode activity as confirmed by the slip system transition from ½ <110>{001} or {110} toward ½<110>{111} observed in hyper stoichiometric UO_{2+x} below 1000 °C [25]. Note that the softer slip plane in UO_2 fluorite is not the densest as classically observed in metals with a face-centered cubic structure. This property has been attributed to the ionic structure of UO_2 for which the primary slip planes (*i.e.,* {001}) are the ones minimizing the electrostatic energy rather than the elastic energy.

For temperatures higher than 1150°C, details on isolated dislocations are rather poor. Usually, for temperatures higher than $0.4T_m$ (T_m*:* melting temperature, 2 847 ± 30°C for UO_2 [36]), climb being effective; and in the literature, several authors have supposed that dislocation climb is involved during plastic deformation. Yust *et al*. [28] suggest that above T_t (a high temperature transition which depends on the strain rate and ranges between 1400 and 1700°C for $\dot{\varepsilon}$ between 2.5×10^{-5} and 2.5×10^{-3} s^{-1}), dislocation climb become favorable. They also observed dislocation network formation and grain boundary sliding. However, climb mechanism has never been clearly identify and no dedicated analysis about elementary processes of dislocation motion can be found.

This work focuses on the dislocation microstructure obtained after uniaxial compression tests of polycrystalline UO_2 pellets at $\dot{\varepsilon} = 10^{-4}$ s^{-1} and T = 1550°C using TEM. Three compression tests were conducted up to various final strains, *c.a.* 1.7, 8.1 and 22% before the sample get quenched in a Ar/H_2(5%) atmosphere at 30°C/min. Even if the cooling rate is relatively rapid, the specific shape of some of the dislocation lines might be expected to vary slightly as a result of stress relaxation.

Further experimental details can be found in Part 1 of the Supplementary Materials.

The strained samples present different features: mainly isolated dislocations (not involved in networks) and groups of dislocations forming different types of networks, corresponding to sub-grain boundaries. These latter will be characterized in detail in a further work.

The three samples present similar non-uniform distributions of dislocations, as illustrated in Figure 1 where, overall, no preferential crystallographic direction was noticed. Dislocations are often attached to porosities or near grain/sub-grain boundaries, as observed by Yust *et al*. at the same temperature [28]. There is TEM evidence that confirm that stress concentration at some pores and grain boundaries sometimes become high enough to nucleate dislocations. Yust *et al*. [28] observed Frank-Read sources near grain boundaries as well as small dislocation loops near porosities that could be the result of the 'pinching off' of dislocations emerging from them. Some dislocation reactions and entanglements are also observed. Here, the dislocation microstructure is particularly different from those observed at lower temperatures as, *e.g.* in [26][27], where dipoles and long lines that present sharp changes from one <100> direction to another one, typical of a lattice friction regime, were characterized.

In the following, we use the Steeds *et al.* [37] method to measure the dislocation density ρ in case of heterogeneous dislocation distribution within the grain while the sample thickness is determined using the fringe method [38]. The density is averaged over 5 grains since it varies slightly from one grain to another one. We have measured $\rho_{1.7\%} = 1.9 \pm 0.3 \times 10^{12}$ m^{-2}, $\rho_{8.1\%} = 2.4 \pm 0.3 \times 10^{12}$ m^{-2} and $\rho_{22\%} = 2.9 \pm 0.4 \times 10^{12}$ m^{-2}. Considering uncertainties (mainly related to thickness variations within the grains), the dislocation density only slightly increases with strain. These small variations suggest an important restoration stage, possibly induced by the vicinity of free surfaces, the presence of grain boundaries or the formation of dislocation walls (weakly disoriented grain boundaries or sub-grain boundaries) where moving dislocations could annihilate thank to active slip, cross-slip and/or climb.

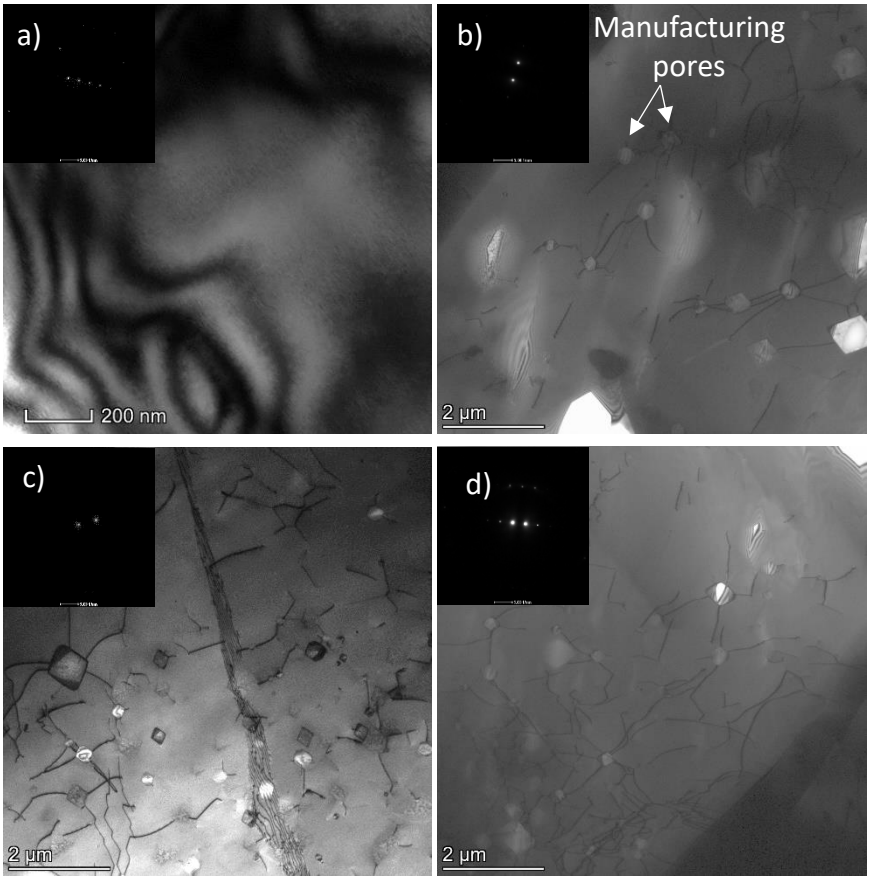

Figure 1. Bright field (BF) TEM images of (a) a fresh UO_2 sample and of dislocations induced by compression tests at 1550°C up to a final strain of (b) 1.7%, (c) 8.1%, (d) 22%, with a constant strain

rate of 10^{-4} s^{-1}. The diffraction vectors are oriented along one of the cubic UO_2 <111> directions for (a), <220> directions for (b,c) and <200> directions for (d). Images were recorded at room temperature.

In order to determine the dislocation motion mechanism, tilt experiments combined with stereographic analysis were performed, as described in more details in [39][40]. Two mechanisms were identified.

First, in the sample strained up to 1.7%, a portion of dislocation loop is studied using different diffraction vectors ***g*** by tilting the sample (*cf.* Figure 2(a)). We assume that (i) the dislocation is part of a loop that was truncated during the thin foil preparation and that (ii) the plane defined by the loop is the plane in which the dislocation has moved. The imaginary line between the two extremities of the line is the intersection of this plane with the thin foil surface. When tilting the sample, the width of projection of the dislocation loop portion changes. When the loop plane is parallel to the electron beam, the projection of the loop appears rectilinear. In this case, the projection of the loop appears rectilinear at α = -38°. The trace of the loop portion plane at -38° is reported on the stereographic representation (*cf.* Figure 2(b)). This trace is close to a plane of high Miller indexes (here close to (382)).

In parallel, using the extinction criterion $\boldsymbol{g}.\boldsymbol{b} = 0$, a Burgers vector $\boldsymbol{b} = \frac{1}{2}[0\bar{1}1]$ is determined. Details on the dislocation invisibility criterion are provided in Part 2 of the Supplementary Materials. This Burgers vector ***b*** forms any angle with the dislocation segment. This latter has thus a dominant mixed character.

The Burgers vector is also reported on the stereographic representation (*cf.* Figure 2(b)) as compared to the dislocation motion plane orientation. In this example, the motion plane is not perpendicular to the Burgers vector and, thus, does not correspond to a pure climb plane (here $(0\bar{2}2)$). Furthermore, the motion plane does not contain the Burgers vector and thus deviates from the closest glide planes ((111) or (022)) which confirms that the dislocation does not move neither by pure nor cross slip only. Its orientation deviates from the (111) and (022) glide planes by around 31° and 36°, respectively. These deviations are higher than the experimental uncertainty associated to this kind of measurement, and which is evaluated to ±5°. Note that the slip plane (022) runs throughout the loop portion trace and could thus correspond to the original dislocation slip plane, from which the dislocation edge component could have escaped by climb. The dislocation displacement process being only partially associated to dislocation climb, one could refer it to as “mixed climb”, as suggested in [40]. During this process, the dislocation moves in mixed climb planes close, but clearly distinct, from slip and climb planes by a combination of glide and climb events (*cf.* Figure 2(c)). For a loop portion, this mechanism requires the nucleation and climb of a jog which are processes related to the emission or absorption of point defects. The resulting plane does not contain the Burgers vector but is neither perpendicular to it. According to [39], this mechanism is favored by high temperatures and low stresses. Moreover, the higher the temperature is, the greater the deviation of the slip plane towards the pure climb plane is. This mechanism allows a dislocation to escape from its original slip plane in which it is submitted to frictional forces, and it could be more favorable than pure climb at intermediate temperatures (in this study $T\ (°C) = 0.54T_m$), since it requires fewer atoms to diffuse. It is then possible that the dislocation studied here moves by mixed climb, as pure glide in the {110} planes remains difficult at 1550°C. Indeed, according to the literature, in stoichiometric UO_2, $T_a^{\{001\}}$ and $T_a^{\{110\}}$ are about 1477 and 1977°C [34], respectively. As a consequence, at 1550°C, dislocations are believed to glide in a viscous manner (athermal regime) in the ½<110>{001} slip system and into a more thermally-activated fashion in ½<110>{110}.

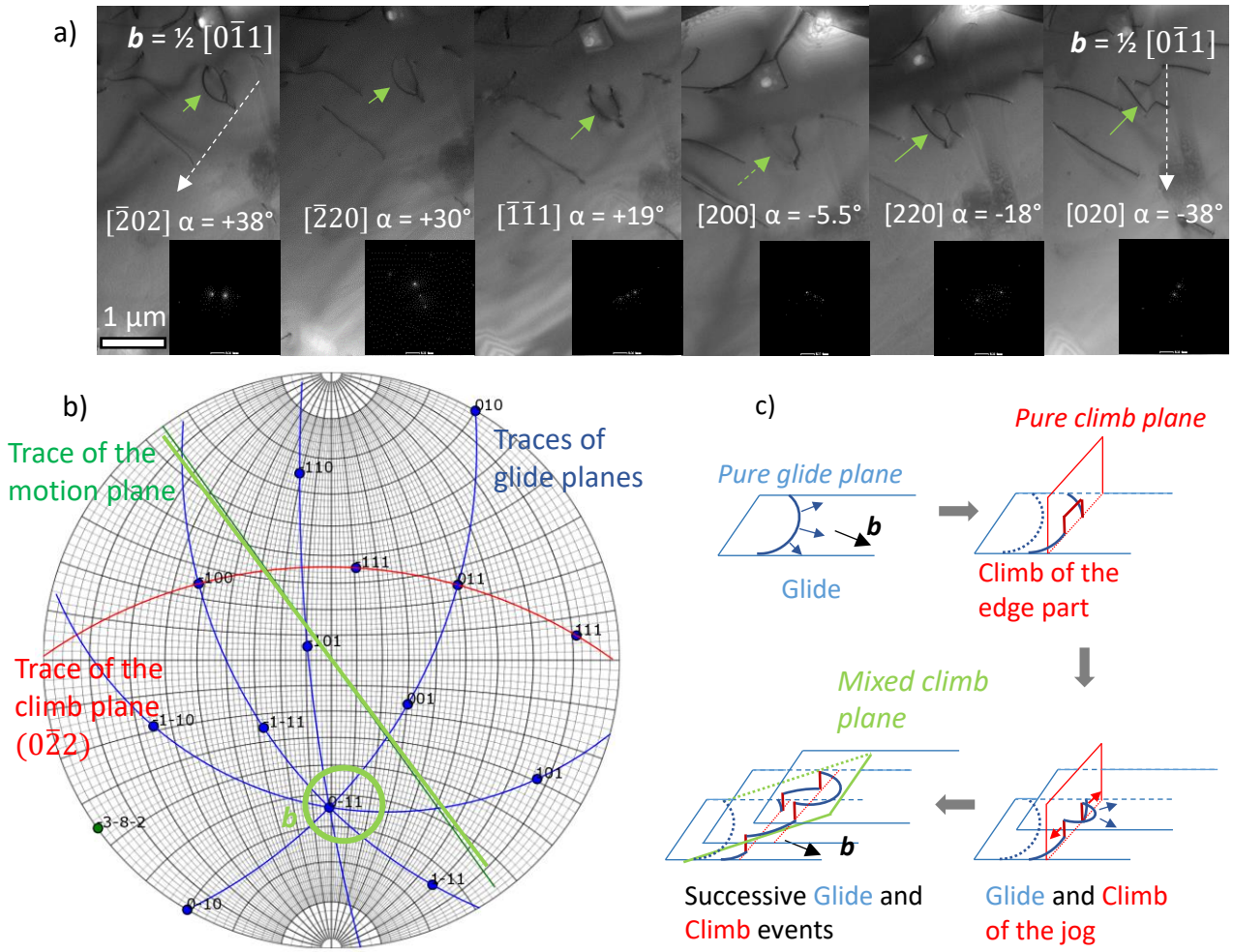

Figure 2. (a) BF TEM images of a dislocation, indicated by a green arrow, from the 1.7% strained UO_2 pellet. Images were recorded at room temperature. The Burgers vector is reported. Dotted lines indicate that the vector is not contained in the image plane. On this series of images the width of projection of this dislocation loop portion changes with the tilt angle α. Diffraction patterns indicate the directions of the different diffraction vectors oriented along one of the cubic UO_2 directions. (b) Stereographic representation associated to the image at α = -38° obtained with the Stereoproj software [41]. The Burgers vector is circled and the motion plane trace is reported in green, the climb plane trace is reported in red and the slip plane traces in blue. (c) Diagram illustrating the mixed climb mechanism for a loop portion.

In the next example, a screw segment of a dislocation line has been studied in the sample strained at 1.7%. Using the extinction criteria, it exhibits a Burgers vector along the $[\bar{1}01]$ direction. The segment appears curved between -30° and +40.5°, and straight at -44° (*cf*. Figure 3(a)). Using the methodology explained above, the Burgers vector belongs to the displacement plane and the latter therefore corresponds to a slip plane (*cf*. Figure 3(b)). In that case, the motion plane does not correspond to a crystallographic slip plane. This result can be due to a succession of cross-slip events between two (or more) slip planes, as illustrated in Figure 3(c).

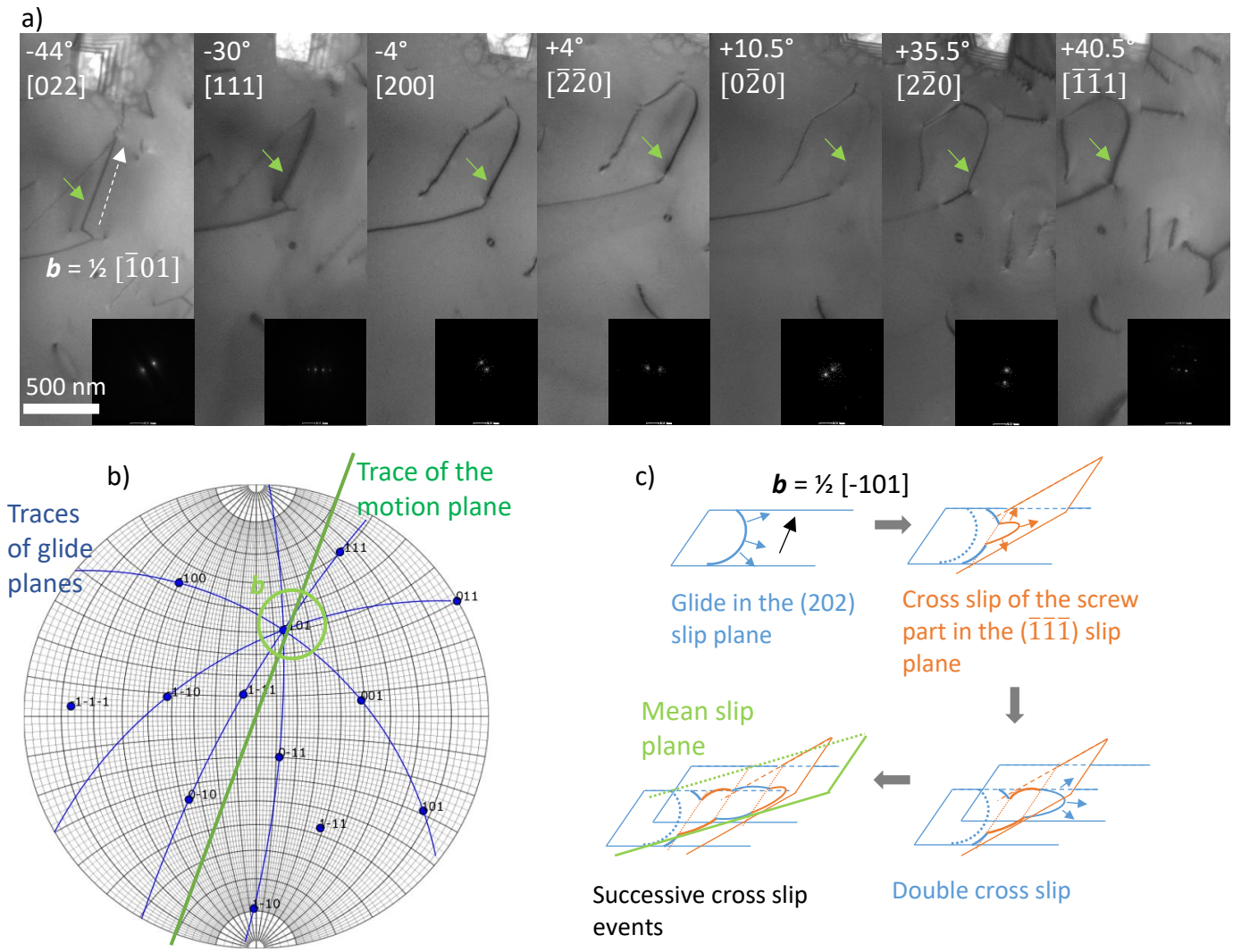

Figure 3. (a) Series of BF TEM images of a dislocation, indicated by green arrows, from the 1.7% strained UO_2 pellet. Diffraction patterns indicate the directions of the different diffraction vectors oriented along one of the cubic UO_2 directions. Images were recorded at room temperature. (b) Stereographic representation associated to the image at α = -44° obtained with the Stereoproj software. The Burgers vector is circled and the motion plane trace is reported in green, the glide plane traces are reported in blue. (c) Diagram illustrating multiple cross slips.

In the last example, we performed a 3D reconstruction of a part of the sample strained at 22%, following the method described in the Part 1 of the Supplementary Materials and in [42]. Here the dislocation curved segment could not be positioned edge-on using the conventional procedures shown above due to limitation in tilt angles of the sample holder (± 45°) which justifies the reconstruction. Tilt experiment combined with stereographic analysis performed on this 3D reconstruction allowed us to study several dislocations near a sub-grain boundary. In Figure 4 (a-d) several dislocations, stopping at a sub-grain boundary, can be seen. Using the extinction criterion, all Burgers vectors are found to be parallel to the $[0\bar{1}1]$ direction. The lines present a dominant edge component. Supplementary Movie 1 focuses on some lines indicated by a red rectangle in Figure 4 (e). In Figure 4 (f-j), a curved dislocation segment is observed for different α tilt angles. The dislocation segment appears rectilinear at around α = +75°, and has thus moved in a $(0\bar{2}\bar{2})$ plane as shown on the associated stereographic representation (*cf.* Figure 4 (k)). Note that such elevated α tilt angles could not be achieved with TEM sample holders, conforming the need for a tomography experiment as shown here. Alternatively, in some configurations a sinusoidal function could have been used to fit the variation in the projection

width of the dislocation loop portion as a function of the α tilt angle [40]. The Burgers vector is also reported on the stereographic representation. In this example, the motion plane $(0\bar{2}\bar{2})$ contains the Burgers vector and thus corresponds to a slip plane. Therefore, this dislocation segment, actually moves by pure glide, without climb contribution. Two others dislocations were studied in the same area and found to move by mixed climb.

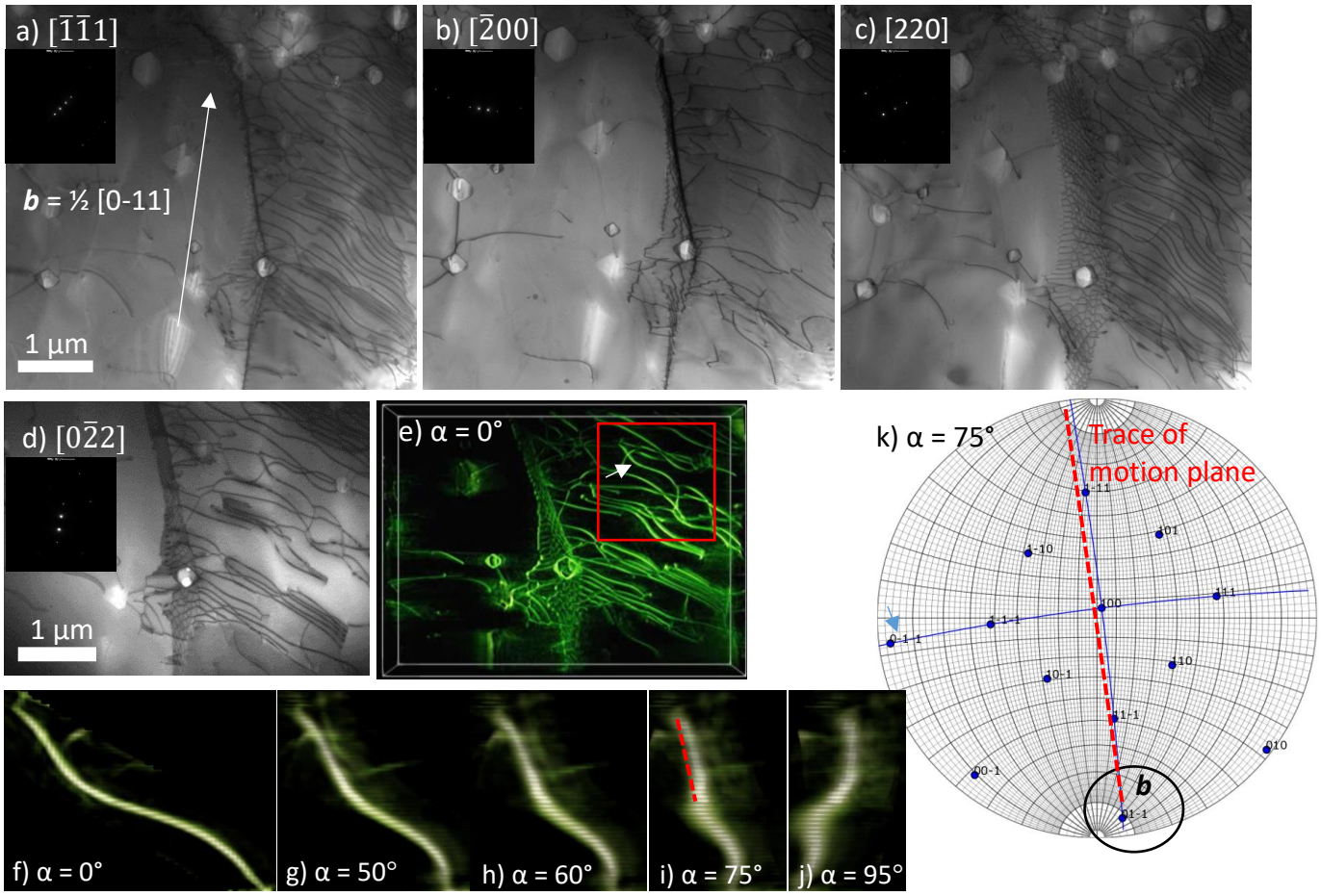

Figure 4. (a-d) BF TEM images of dislocations stopping on a sub-grain boundary obtained at different diffraction vectors, from the 22% strained UO_2 pellet. On image (b) the lines are out of contrast. The Burgers vector is indicated on (a) along the $[0\bar{1}1]$ direction. Diffraction patterns indicate the directions of the different diffraction vectors oriented along one of the cubic UO_2 directions. Images were recorded at room temperature. (e) 3D reconstruction, using the diffraction vector of (d), visualized using Tomviz. (f-j) On this series of images a part of a curved dislocation segment is followed with the α tilt angle. (k) Stereographic representation associated to image (i). The Burgers vector is circled and the motion plane trace is shown by a red dotted line. It corresponds to $(0\bar{2}\bar{2})$. See also Supplementary Movie 1.

Thirteen dislocations were studied using tilt experiments. Nine of them move by a mixed climb mechanism; that is in planes that neither contain the Burgers vector nor are perpendicular to it. Four of them glide, mainly in the {110} type planes, and sometimes involving cross slip. Surprisingly, no slip is observed in {100} type planes. However, several aspects need to be considered:

- The combination of tilt experiments and stereographic analysis can only be applied to a limited number of objects. Indeed, the dislocation must be curved and able to be positioned edge on. The number of favorable situations is therefore particularly limited.

- The final chemical etching used to prepare the thin foils is more or less effective, depending on the orientation of the grains. The studied grains are mainly oriented along [100] or [110] directions that could favor some slip systems. However as the applied stress is relatively low, the effect of internal stresses and other grains may be predominant which makes Schmid factor irrelevant for predicting system activation in polycrystalline pellets [43].

At low temperature in UO_2, dislocation motion is generally restricted to stress-induced glide, where sinter pores and grain boundaries are the main obstacles. As a result, dislocation dipoles, structures resembling superjogs, dislocation lines with sharp changes from a <100> direction to another one (forming cups), and entangled dislocation clusters were observed [26][27]. For higher temperatures (and/or lower strain rate), cross-slip and climb become favorable and hexagonal networks and more complex substructures occur [11][26][28]. In metal systems, the climb of edge dislocations together with the glide of jogged-screw dislocations both contribute as rate-controlling processes at high-temperature. However, Nadeau [44] ruled out both processes when applied to UO_2 as they do not account for the plastic anisotropy he observed in single crystals. Thus, Nadeau proposed that plastic deformation at high-temperature is controlled by the activation of secondary slip systems (*i.e.*, ½<110>{110}). In polycrystalline UO_2, Yust *et al.* [28] suggest grain boundary sliding also contributes to the total strain, in addition to dislocation-induced deformation within the grains. Recently, DDD and CPFEM simulations have emphasized the role played by the composite slip process *i.e.*, the tendency for dislocation density transfer and annihiling in between ½<110>{001}, ½<110>{110} and ½<110>{111} slip systems with same Burgers vectors, in UO_2 at 1600 K [35]. Also, Borde *et al.* have confirmed the occurrence of cross-slip of screw dislocation portions under heterogeneous stress field using MD simulation, in the same temperature range [45].
In this study, we confirm that the movement of dislocations is more complex than pure glide or pure climb for a temperature of about 1550°C and a strain rate of 10^{-4} s^{-1}. The studied dislocations move through mixed climb, as pure glide in the {110} planes could remain difficult at 1550°C, which gives dislocations a higher degree of mobility. We also evidence dislocations that move by the succession of cross-slip events between at least two slip planes. Therefore, both mechanisms (climb and glide of jogged screw dislocations) are thus expected to be involved in the dislocation motion, which will impact the rate controlling parameters.

To summarize, in the three samples, strained at 1550°C up to the final strain values of 1.7%, 8.1% and 22%, isolated dislocations (not involved in sub-grain boundaries) are observed using TEM. In their large majority, these dislocations do not lie along any preferential crystallographic direction and are rather connected to porosities, or located near grain/sub-grain boundaries where they often begin to interact or are tangled. It was shown by conventional tilt experiments that they can move by two mechanisms: glide, mainly in the ½ <110>{110} system and sometimes involving cross slip, and by a mixed mechanism involving climb, called mixed climb. During this process, the dislocation moves in mixed climb planes close, but clearly distinct, from pure slip and climb planes by a combination of glide and climb events. We can thus state that at 1550°C the mobile dislocations can sometimes leave their original slip plane by climb, which is a way to spread the deformation in the crystal, and not only on crystallographic slip planes, and that enables dislocations to move more freely. Furthermore, this mixed climb mechanism could be more favorable than pure climb at intermediate temperatures (in this study $T\,(°C) = 0.54T_m$), since it requires fewer atoms to diffuse. The study of a sample deformed at higher temperature (or lower strain rate) would enable us to establish whether pure climb would become more favorable. This work on dislocation motion mechanisms will thus contribute to improve the modelling of the high temperature viscoplastic behavior of the UO_2 fuel at the nanoscale by taking into account more realistic dislocation displacement mechanisms.

Acknowledgments

The authors would like to thank Dr. Caillard (CNRS/CEMES) for interesting discussions regarding dislocation motion mechanisms. This work benefited from a support of the Cross-cutting basic research program (RTA Program) of the CEA Energy Division.

References

[1] B. Michel, C. Nonon, J. Sercombe, F. Michel & V. Marelle (2013), Simulation of Pellet-Cladding Interaction with the PLEIADES Fuel Performance Software Environment, Nuclear Technology, 182:2.
[2] Armstrong, W. M., Irvine, W. R., & Martinson, R. H. (1962). Creep deformation of stoichiometric uranium dioxide. Journal of Nuclear Materials, 7(2), 133-141.
[3] M.S. Seltzer, A.H. Clauer, B.A. Wilcox, The stress dependence for high temperature creep of polycrystalline uranium dioxide, J. Nucl. Mater. 34 (1970), 351.
[4] Scott, R., Hall, A. R., & Williams, J. (1959). The plastic deformation of uranium oxides above 800°C. Journal of Nuclear Materials, 1(1), 39 48.
[5] Seltzer, M.S., Clauer, A.H., Wilcox, B.A., Influence of stoichiometry on compression creep of polycrystalline UO_{2+x}, J. Nucl. Mater. 44 (1972), 331.
[6] B. Burton, G. L. Reynolds & J. P. Barnes, The influence of grain size on the creep of uranium dioxide, J. Mater. Sci. 8 (1973), 1690.
[7] Y. Guerin, Etude par compression a hautes temperatures de la deformation plastique du bioxyde d'uranium polycristallin, J. Nucl. Mater. 56 (1975) 61.
[8] B. Burton, G.L. Reynolds, The diffusional creep of uranium dioxide: its limitation by interfacial processes, Acta. Metall., 21 (1973), 1073.
[9] Bohaboy, P. E., Asamoto, R. R., & Conti, A. E. (1969). Compressive creep characteristics of stoichiometric uranium dioxide. U.S. Atomic Energy Commission.
[10] T.G. Langdon, Creep mechanisms in stoichiometric uranium dioxide, J. Nucl. Mater. 38 (1971), 88.
[11] Dherbey, F., Louchet, F., Mocellin, A., Leclercq, S., 2002. Elevated temperature creep of polycrystalline uranium dioxide: from microscopic mechanisms to macroscopic behaviour. Acta Materialia 50, 1495–1505.
[12] Salvo, M., Sercombe, J., Ménard, J.-C., Julien, J., Helfer, T., Désoyer, T., 2015. Experimental characterization and modelling of UO2 behavior at high temperatures and high strain rates. Journal of Nuclear Materials 456, 54–67.
[13] J. Nadeau, Dependence of flow stress on nonstoichiometry in oxygen-rich uranium dioxide at high temperatures, J. Am. Ceram. Soc., 52 (1) (1969), p. 1
[14] Wolfe, R. A., & Kaufman, S. F. (1967). Mechanical properties of oxide fuels (WAPD-TM--587, 4511674; p. WAPD-TM--587, 4511674).
[15] Chung, T. E., & Davies, T. J. (1979a). The superplastic creep of uranium dioxide. Journal of Nuclear Materials, 79(1), 143 153.
[16] Chung, T. E., & Davies, T. J. (1979b). The low-stress creep of fine-grain uranium dioxide. Acta Metallurgica, 27(4), 627 635.
[17] Vivant-Duguay, C. (1998). Contribution à l'étude du fluage du dioxyde d'uranium : Rôle des activateurs de croissance cristalline. Thèse - Université de Lyon.
[18] Colin, C. (2003). Etude du fluage du dioxyde d'uranium : Caractérisation par essais de flexion et modélisation mécanique. Thèse - Ecole Nationale Supérieure des Mines de Paris.
[19] Garcia, P., Miard, A., Helfer, T., Parise, J.-B., Iltis, X., & Antou, G. (2021). The effect of oxygen partial pressure on dislocation creep in polycrystalline uranium dioxide. Journal of European Ceramic Society, 41(3), 2124-2133.
[20] Ndiaye, A. (2012). Microstructures d'UO2+x à propriétés pilotées : Compréhension des mécanismes d'élaboration et du comportement mécanique en température. Thèse - Université de Grenoble.
[21] Sawbridge, P.T., Sykes, E.C., 1971. Dislocation glide in UO2 single crystals at 1600°K. The Philosophical Magazine: A Journal of Theoretical Experimental and Applied Physics 24, 33–53.

[22] Seltzer, M. S., Clauer, A. H., & Wilcox, B. A. (1972). The influence of stoichiometry on compression creep of uranium dioxide single crystals. Journal of Nuclear Materials, 44(1), 43 56.
[23] J.M. Lefebvre, Contribution à l'étude de la déformation plastique d'une céramique de structure fluorite : le bioxyde d'uranium, Faculté des sciences de Poitiers (1976).
[24] E.J. Rapperport and A.M. Huntress, Deformation Modes of Single Crystal Uranium Dioxide from 700°C to 1900°C, NMI-1242 Metallurgy and Ceramics (1960).
[25] R.J. Keller, T.E. Mitchell, A.H. Heuer, Plastic deformation in nonstoichiometric UO2+x single crystals – I. Deformation at low temperatures, Acta metallica, Vol.36, No.4, pages 1061-1071, 1988.
[26] Alamo, A., Lefebvre, J.M., Soullard, J., 1978. Deformation plastique du bioxyde d'uranium: Observation des sous-structures de dislocations. Journal of Nuclear Materials 75, 145–153.
[27] Yust, C.S., McHARGUE, C.J., 1969. Dislocation substructures in deformed uranium dioxide single cristals. Journal of Nuclear Materials 31, 121–137.
[28] Yust, C.S., Roberts, J.T.A., 1973. On the observation of lattice and grain boundary dislocations in UO2 deformed at high temperatures. Journal of Nuclear Materials 48, 317–329.
[29] J.F. Byron. The yield and flow of single crystals of uranium dioxide, J. Nucl. Mat. 28 (1) (1968) 110-114.
[30] Fossati, P., Van Brutzel, L., Devincre, B., 2013. Molecular dynamics simulation of dislocations in uranium dioxide. Journal of Nuclear Materials 443.
[31] Borde, M., Freyss, M., Bourasseau, E., Michel, B., Rodney, D., Amodeo, J., 2023. Atomic-scale modeling of ½<110>{001} edge dislocations in UO2: Core properties and mobility. Journal of Nuclear Materials 574, 154157.
[32] Lunev, A.V., Kuksin, A.Yu., Starikov, S.V., 2017. Glide mobility of the 1/2[1 1 0](0 0 1) edge dislocation in UO2 from molecular dynamics simulation. International Journal of Plasticity 89, 85–95.
[33] Lunev, A.V., Starikov, S.V., Aliev, T.N., Tseplyaev, V.I., 2018. Understanding thermally-activated glide of 1/2〈110〉{110} screw dislocations in UO2 – A molecular dynamics analysis. International Journal of Plasticity 110, 294–305.
[34] Portelette, L., Amodeo, J., Madec, R., Soulacroix, J., Helfer, T., Michel, B., 2018. Crystal viscoplastic modeling of UO2 single crystal. Journal of Nuclear Materials 510, 635–643.
[35] Madec, R., Portelette, L., Michel, B., Amodeo, J., 2023. Plastic anisotropy and composite slip: Application to uranium dioxide. Acta Materialia 255, 119016.
[36] Juan J Carbajo, Gradyon L Yoder, Sergey G Popov, Victor K Ivanov, A review of the thermophysical properties of MOX and UO2 fuels, Journal of Nuclear Materials, Volume 299, Issue 3, 2001, p.181-198.
[37] Steeds J. W., 1966. Dislocation arrangement in copper single crystals as a function of strain. Proceedings of the Royal Society of London. Series A. Mathematical and Physical Sciences 292, 343–373.
[38] Williams, D.B., Carter, C.B., 2009. Transmission Electron Microscopy: A Textbook for Materials Science, 2nd ed. Springer US.
[39] Couret, A., Monchoux, J.-P., Caillard, D., 2019. On the high creep strength of the W containing IRIS-TiAl alloy at 850 °C. Acta Materialia 181, 331–341.
[40] Malaplate, J., Caillard, D., Couret †, A., 2004. Interpretation of the stress dependence of creep by a mixed climb mechanism in TiAl. Philosophical Magazine 84, 3671–3687.
[41] Mompiou, Frédéric, Stereoproj, (2018). doi:10.5281/zenodo.1434934.
[42] J.P. Monchoux, D. Ferry. Habit planes of climbing and gliding dislocations in TiAl determined in three dimensions by electron tomography. Scripta Materialia 236 (2023) 115679.
[43] Kawano, Y., Sato, M., Mayama, T., Mitsuhara, M., Yamasaki, S., 2020. Quantitative evaluation of slip activity in polycrystalline α-titanium considering non-local interactions between crystal grains. International Journal of Plasticity 127, 102638.
[44] J.S. Nadeau, Dependence of Flow Stress on Nonstoichiometry in Oxygen-Rich Uranium Dioxide at High Temperatures, J. Am. Ceram. Soc., 52 (1969), p. 1.
[45] Borde, M., Dupuy, L., Pivano, A., Michel, B., Rodney, D., Amodeo, J., 2023. Interaction between 1/2<110>{001} dislocations and {110} prismatic loops in uranium dioxide: Implications for strain-hardening under irradiation. International Journal of Plasticity 168, 103702.